# High-Fat High-Sucrose Diet Leads to Dynamic Structural and Inflammatory Alterations in the Rat Vastus Lateralis Muscle

**Kelsey H. Collins, B.S.[1,2,‡] khmcolli@ucalgary.ca**

**David A. Hart, Ph.D.[2,4] hartd@ucalgary.ca**

**Raylene A. Reimer, Ph.D.[1,3] reimer@ucalgary.ca**

**Ruth A. Seerattan B.Sc. [1] rseerattan@kin.ucalgary.ca**

**Christine W. Banker Ph.D. [1] chris.waters@ucalgary.ca**

**Scott C. Sibole, M.Sc. [1,2] ssibole@ucalgary.ca**

**Walter Herzog, Ph.D.[1,2] wherzog@ucalgary.ca**

[1]Human Performance Laboratory, University of Calgary, AB, Canada

[2]McCaig Institute for Bone and Joint Health, University of Calgary, AB, Canada

[3]Department of Biochemistry and Molecular Biology, University of Calgary, AB, Canada,

[4]The Centre for Hip Health & Mobility, Department of Family Practice, University of British Columbia, Vancouver, BC, Canada

‡Corresponding Author

**Corresponding Author: Kelsey Collins**

2500 University Drive NW Calgary, AB
Email: khmcolli@ucalgary.ca
Phone: 403-801-6932
Fax: 403-284-3553

**Author Contributions:** KHC was responsible for design of the study, execution of the study, data collection, data analysis, interpretation of data, drafting the manuscript, revising the manuscript and approving the final submitted version. DAH was responsible for data analysis, interpretation of data, drafting the manuscript, revising the manuscript, and approving the final submission. RAR contributed to design of the study, analysis and interpretation of data, revising the manuscript and approving the final submitted version. CWB contributed to design of the study, data collection, manuscript drafting and approving the final submission. SCS contributed to software development and data analysis, revising the manuscript, and approved the final submission. WH contributed to study design, interpretation of the data, writing the manuscript, revising the manuscript, and approving the final submission.

**Wordcount: 4151 words**

**Competing Interests: All authors declare no conflict of interest.**

**Abstract**

The influence of obesity on muscle integrity is not well understood. The purpose of this study was to quantify structural and molecular changes in the rat vastus lateralis (VL) muscle as a function of a 12-week obesity induction period and a subsequent adaptation period (additional 16-weeks). Male Sprague-Dawley rats consumed a high-fat, high-sucrose (DIO, n=40) diet or a chow control-diet (n=14). At 12-weeks, DIO rats were grouped as prone (DIO-P, top 33% of weight change) or resistant (DIO-R, bottom 33%). Animals were euthanized at 12-weeks or 28-weeks on the diet. At sacrifice, body composition was determined and VL muscles were collected. Intramuscular fat, fibrosis, and CD68+ cells were quantified histologically and relevant molecular markers were evaluated using RT-qPCR. At 12- and 28-weeks post obesity induction, DIO-P rats had more mass and body fat than DIO-R and chow rats ($p<0.05$). DIO-P and DIO-R rats had similar losses in muscle mass, which were greater than those in chow rats ($p<0.05$). mRNA levels for MAFbx/atrogin1 were reduced in DIO-P and DIO-R rats at 12- and 28-weeks compared to chow rats ($p<0.05$), while expression of MURF was similar to chow values. DIO-P rats demonstrated increased mRNA levels for pro-inflammatory mediators, inflammatory cells, and fibrosis compared to DIO-R and chow animals, despite having similar levels of intramuscular fat. The down-regulation of MAFbx/atrogin1 may suggest onset of degenerative changes in VL muscle integrity of obese rats. DIO-R animals exhibited fewer inflammatory changes compared to DIO-P animals, suggesting a protective effect of obesity resistance on local inflammation.

***Keywords:*** Sarcopenic Obesity, Intramuscular Fat, Rat, Systemic Inflammation, Vastus Lateralis

## Introduction

Obesity is associated with a variety of co-morbidities and chronic diseases[1]. The systemic metabolic implications of obesity include chronic-low level inflammation, which may affect the integrity and function of tissues[2], and may lead to complications after orthopedic surgery[3]. Muscle is a vulnerable tissue in a chronic low-level inflammatory environment as it is highly plastic and undergoes regular remodeling[4]. As muscle is a key site for glucose storage and utilization, increased intermuscular adipose tissue deposits are positively correlated with insulin resistance[5], and increase with obesity[6,7]. The mechanical, inflammatory, and metabolic link between obesity and musculoskeletal health is still unclear[1].

Acute muscle atrophy is associated with an up regulation of muscle RING-finger protein-1 (MuRF) and MAFbx/atrogin-1 (MAFbx), two muscle-specific E3 ubiquitin ligases that are universally expressed across denervation, hindlimb suspension, and casting atrophy models[8]. However, aging animals have demonstrated a down regulation of MAFbx and MuRF compared to young animals[9]. These data suggest that these atrophy-related factors may behave differently in acute versus chronic stages of muscle loss[10]. In addition, it has been suggested that MAFbx and MuRF are not altered with a high fat diet[11]. However, confirming these findings in a preclinical model of high-fat high-sucrose (HFS) diet-induced obesity may elucidate previously undetected structural and molecular changes in muscle with metabolic dysfunction[12].

Furthermore, a HFS diet leads to obesity prone and obesity resistant phenotypes in Sprague-Dawley rats[13]. We demonstrated that after a 12-week obesity induction and a subsequent 16-week adaptation period, obesity resistant animals are similar in mass but higher in body fat compared to lean chow diet control animals at both time points[12]. Moreover, we have

observed differential rates of metabolic osteoarthritis progression in these obesity prone and obesity resistant animals after a 12-week obesity induction period[14]. Obesity prone and obesity resistant animals have similar serum inflammatory profiles[12,14]. Furthermore, this model presents a unique opportunity to evaluate adiposity and muscle-related changes in the presence of metabolic disturbance, while body mass is conserved.

The purpose of the present study was to quantify changes in the structural and molecular integrity of the rat vastus lateralis (VL) muscle as a function of obesity following a HFS obesity induction period (12-weeks) and a subsequent adaptation period (additional 16-weeks) in obesity prone and obesity resistant Sprague-Dawley rats.

## Methods

Fifty-four male 8-12 week old male Sprague-Dawley Rats were individually housed on a 12/h dark/light cycle. Sample size calculations are reported elsewhere[14]. Animals were randomized into either the HFS diet-induced obesity group (DIO, 40% of total energy as fat, 45% of total energy as sucrose, n=40, **custom Diet #102412, Dyets, Inc,**)[12,14], or the standard chow low fat diet group (chow, 12% fat, 3.7% sucrose, n=14, **Lab Diet 5001**) for a 12-weeks *ad libitum*. All experiments were approved by the University of Calgary Life and Environmental Sciences Animal Care Committee. Throughout the obesity induction period, animal mass was recorded weekly. After 12-weeks, DIO animals were stratified into tertiles according to their change in body mass over 12-weeks and termed obesity prone (DIO-P, top 33% of animals by change in body mass, n=13) or obesity resistant (DIO-R, bottom 33% of animals by change in body mass, n=13), which was determined *a priori*. The middle tertile group was not further considered. Half of the animals from each group (DIO-P, n=6; DIO=R, n=6; chow, n=7) were

euthanized after the obesity induction period, while the remaining animals were followed for an additional 16 weeks, or 28 weeks in total (36-40 weeks old, DIO-P, n=7; DIO=R, n=7; chow, n=6). Primary outcomes included body fat, VL histology, and VL muscle mass. Secondary outcomes included VL qPCR data.

**Body Composition.** Animals were euthanized by barbiturate overdose (Euthanyl®, MTC Animal Health Inc., Canada). Immediately after sacrifice, body composition was measured using Dual Energy X-ray Absorptiometry and analyzed with software for small animal analysis (Hologic QDR 4500; Hologic, USA).

**Histology**.

*Slide preparation:* At sacrifice, the right VL muscle was harvested and whole muscle wet weight was measured (g). Muscles were immediately flash frozen in liquid nitrogen and stored at -80°C. A slice from the mid-belly of the tissue was cut and mounted in OCT compound and 10 micron serial cross-sections were prepared using a cryostat at -25°C. Slides were stored overnight at -25°C before staining.

*Oil Red O Staining:* Slides were stained with Oil Red O (ORO) working solution prepared from 3 parts ORO stock: 2 parts distilled water and refrigerated at 4°C for 10 minutes before use. ORO stock solution was made by adding 2.5g Oil Red O (Sigma) to 400mL 99% isopropanol (Fisher). Sections were washed in distilled water, quickly dipped in 60% isopropanol, and stained for 20 minutes in the ORO working solution. Slides were then rinsed in 60% isopropanol and then rinsed in distilled water. Sections were counterstained for 1 minute with Harris hematoxylin, rinsed in tap water, and cover-slipped with glycerol jelly.

*Picrosirius staining:* Slides were air dried, immersed in Bouin's fixative solution for 1 hour at 60°C, in a water bath, and then washed in distilled water. Picrosirius red solution was made by adding 0.1g of Sirius red stain from Sigma, to 100ml of a saturated aqueous picric acid (1.3% in water from Sigma). Sections were stained in this solution for 1hr at room temperature. Slides were rinsed in 0.5% acetic acid, dehydrated in 3 changes of 100% ethanol, cleared in xylene and mounted with DPX mounting media.

*Stain Quantification:* Sections were imaged at 100x magnification on an Olympus BX53 light microscope and analyzed using a custom MatLab program. The intensity of each stain was averaged across each muscle section (30-50 frames/animal).

*Exploratory Fibre Area Measurements:* Muscle fibres were segmented from one picrosirius red-stained slide/animal using custom software developed in C++ and Python and an open-source region competition code[15]. Briefly, the segmentation procedure involved color to grayscale conversion numerically maximizing contrast[16]. Fibre edge probability maps were then generated based on the eigenvalues of the hessian matrix measured across scale-space[17,18], and pixels with a probability higher than 15% were considered as an edge[16]. The binary inverse of these edges served as seeds for the region competition algorithm. The resulting segmentations were user-inspected, and fibre areas of correctly labeled regions were calculated. Sections with >120 labeled fibres were analyzed.

**Immunohistochemistry.**

Slides were fixed in ice cold 100% acetone as described previously[19]. Briefly, sections were blocked with 3% hydrogen peroxide in PBS, followed by 2.5% normal horse serum (Vector Labs, USA). Sections were then incubated with the primary antibody, ED1 mouse anti-rat CD-68+, a marker for pro-inflammatory macrophages (Ad Serotec, USA) at 1:100 dilution overnight at 4°C. The secondary antibody, anti-mouse IgG peroxidase was applied for 30 mins at room

temperature (IMPRESS kit, Vector labs, USA). Sections were incubated in a Cyanine 3 fluorophore, prepared in Tyramide Signal Amplification buffer (PerkinElmer,USA) for 20 mins. DAPI was applied to visualize nuclei and sections were mounted in Vectashield mounting media (Vector Labs, USA). Four images per VL cross-section were obtained using an Olympus FV100 confocal microscope (Japan) using a QImaging Retiga 4000R camera and QCapture Software (Canada) at 200x magnification.

**Vastus lateralis qPCR.** Samples of mid-belly frozen vastus lateralis tissue were powdered at liquid nitrogen temperatures with a Braun Mikro-dismembrator (Braun Biotech International, USA) and total RNA isolated using the TriSpin method[20,21]. qPCR was performed as described previously with an iCycler (BioRad Laboratories Inc, ON) and rat-specific primers were validated for the molecules listed in Supplementary Table 1[21]. All assessments were performed in duplicate under optimal conditions that conformed to qPCR criteria.

**Statistical Comparisons.** All groups were compared to their respective chow control group within time points, and DIO-P animals were compared to DIO-R within time points. Levene's test for equality of variance was conducted on all outcomes. If equality of variance was rejected ($p<0.05$), Kruskal-Wallis non-parametric tests were used to evaluate each outcome between phenotype/diet groups (DIO-P, DIO-R, chow). If equal variance was confirmed, ANOVAs were performed to assess differences between groups. Bonferroni corrections were applied when appropriate (IBM SPSS Statistics 20, $\alpha=0.05$). Statistics were conducted on raw values for mRNA levels, but data are presented as fold change compared to chow control-diet animals.

## Results

***Body Composition, Vastus Lateralis Muscle Mass and Sarcopenia Index***. At both time points assessed, DIO-P animals demonstrated statistically more mass and body fat than the DIO-R and chow animals (*Figure 1A, Figure 1B,* $p<0.05$). At both time points, DIO-P and DIO-R animals had similar decreases in wet VL muscle mass compared to chow-fed control rats (*Figure 2A*, $p<0.05$). When VL mass was normalized to body mass, the sarcopenia index calculated for DIO-P animals was statistically lower for DIO-P animals compared to both DIO-R and chow animals at both time points (*Figure 2B,* $p<0.01$). DIO-R animals also demonstrated statistically lower sarcopenia indices compared to chow at each time point ($p<0.05$), suggesting an induced and sustained muscle loss, despite similar mass when compared to chow.

***Vastus Lateralis Morphological Changes.*** DIO-P and DIO-R animals demonstrated similar levels of ORO staining at both time points, and values were significantly greater than their corresponding chow-fed control (*Figure 3A, Figure 3B,* $p<0.001$). Of note, intramuscular fat was observed between and within fibres.

At 12-weeks, intramuscular fibrosis levels were increased in DIO-P animals compared to DIO-R and chow animals, and DIO-R animals had increased fibrosis compared to chow (*Figure 3C,D*). At 28-weeks, fibrosis was similar between DIO-P and DIO-R animals, which was significantly greater than that detected in chow animals. Similarly, CD68+ cells were increased in DIO-P compared to DIO-R and chow animals at 12-weeks ($p=0.028$), but were similar in DIO-P and DIO-R animals ($p>0.05$), but greater than chow animals, at 28-weeks (*Figure 3E,F*). In a subset of animals, fibre area measurements revealed decreased muscle fibre area in both DIO-P and DIO-R animals compared to chow-fed control animals at both time-points *(Figure 4*).

At 28-weeks, there was a significant negative relationship between body fat and VL mass (*Figure 5A*; r=-0.50, p=0.03), but not at 12-weeks (p=0.10). At both time points, there was a positive relationship between body fat and VL fat (*Figure 5B*; 12-weeks: r=0.79, p<0.001; r=28-weeks: r=0.84, p<0.001). Furthermore, there was a positive relationship between body fat and picrosirius red staining (12-weeks r=0.77, p=0.001; 28-weeks r=0.56, p=0.001), and between VL fat and picrosorius red staining (*Figure 5C;* 12-weeks r=0.73, p=0.001; 28-weeks r=0.63, p=0.003) at both time points.

***Vastus Lateralis Atrophy Marker qPCR Assessments***. Across both time points, mRNA levels for MAFbx were down-regulated in DIO-P and DIO-R animals compared to values for chow-fed animals (*Figure 6*, p<0.05). MuRF expression levels were similar across all animals at 28-weeks (p>0.05).

Conversely, qPCR assessments for a subset of adiopokines and inflammatory markers indicated differences between DIO-P and DIO-R animals, despite similarities in the relative percentage of ORO staining in VL muscle from DIO-P and DIO-R animals. Specifically, at 12-weeks, adiponectin (3-fold increase in DIO-P compared to DIO-R and chow animals, p=0.007, *Table 1*), Monocyte Chemoattractant Protein-1 (MCP-1/CCL2, 2.2-fold increase vs. DIO-R, p=0.02 and 2.5 fold increase vs. chow animals, p=0.008) and Interferon-gamma-inducible protein 10 (IP-10/CXCL-10) mRNA levels were up-regulated in the muscle tissue of DIO-P animals compared to both DIO-R and chow-fed control animals (*Figure7*, p<0.05). DIO-R and chow animals exhibited similar mRNA levels for these markers. Adiponectin, IP-10 and MCP-1 levels were similar to those of chow animals by 28-weeks for DIO-P and DIO-R animals (p>0.05).

Further, a subset of markers assessed exhibited a dose-response relationship with response to obesity. DIO-P mRNA levels for leptin were increased approximately 5-fold compared to DIO-R animals (p=0.01, *Table 1*) and 17-fold in DIO-P animals compared to chow at 12-weeks (p=0.002, Figure 7). DIO-R and chow animals demonstrated similar mRNA levels for leptin. Similarly Interleukin-1β (IL-1β) mRNA levels were up-regulated in DIO-P animals (3.1 fold change versus chow, p=0.007), and also up-regulated in DIO-R compared to chow-fed control animals (1.7 fold versus chow, p=0.022). Additionally, peroxisome proliferator activated receptor gamma (PPARγ), a marker of adipose cell differentiation[22], mRNA levels were increased 1.9-fold in DIO-P animals compared to chow (p=0.02). Insulin-like growth factor-1 (IGF-1) levels were increased 3-fold in DIO-P animals compared to chow (p=0.01). mRNA levels for Leptin, PPARγ and IGF-1 were similar across groups at 28-weeks, while DIO-P animals demonstrated 2.4-fold increased mRNA levels for IL-1β (p=0.01).

## Discussion

In this study, we demonstrated strong associations between body fat and a direct measure of VL intramuscular fat at two time points; immediately post-obesity induction (12-weeks on the diet), and after a further 16-week adaptation period (28-weeks total). Our major findings include 1) similar levels of intramuscular fat across DIO-P and DIO-R animals at both time points; 2) increased fibrosis at 12-weeks in DIO-P compared to DIO-R and chow animals, and increased in DIO-R compared to chow; 3) MAFbx/atrogin1 mRNA levels were down-regulated in all DIO animals at both time points; 4) mRNA levels for a select subset of molecular markers involved in chronic inflammation were differentially up-regulated in DIO-P and DIO-R animals at 12 and 28-weeks.

Although intramuscular fat infiltration observed after the obesity induction period, appears similar in DIO-R and DIO-P animals, fibrosis was increased in 12-week DIO-P animals compared to both DIO-R and chow. As fat is an active endocrine organ[23], these findings highlight the potential implication of intramuscular fat deposits on muscle structure and function, of inflammatory changes within the muscle, and a potential role for muscle inflammation in the development of subsequent pathology (e.g. sarcopenic obesity and/or metabolic osteoarthritis). Relevant to this point, CD68+ cells were quantified, and the results indicated a significantly enhanced presence of pro-inflammatory cells in DIO-P compared to DIO-R and chow animals at 12-weeks. The levels observed here were concordant with previous reports of CD68+ cells in animals following metabolic challenge[24]. Future studies with short time points are needed to understand early changes in intramuscular fat deposition, the obesity response, and the inflammatory changes in muscles and joints prior to the time points assessed in the present studies. Adipose tissue lipid storage is altered with obesity, and adipose tissue fibrosis is considered a hallmark of metabolic alterations [25,26]. Furthermore, insulin resistance is thought to be a consequence of human adipose tissue fibrosis [26]. Cross-talk has been observed between adipose tissue and skeletal muscle during obesity onset[27]. Both mechanically and biologically, infiltration of fat and fibrosis in muscle tissue can compromise function, insulin sensitivity and biological homeostasis within the muscle [25]. However, the determinants of this intramuscular fibrosis, or whether this fibrosis relates to intramuscular adipose tissue deposits, are unclear [25,27].

The findings regarding MAFbx/atrogin1 were surprising, as previous reports have suggested that MAFbx/atrogin1 mRNA levels are unchanged with high fat feeding[11]. MAFbx/atrogin1 is an E3 ligase in the ubiquitin proteasome pathway utilized for protein

degradation in numerous models of skeletal muscle atrophy, and has been shown to be down-regulated with aging. Therefore, the down-regulated expression of MAFbx/atrogin1 at both time points in our study may be an indication of an early onset of sarcopenic-like muscle changes in animals both prone and resistant to obesity. However, MuRF-1 mRNA expression was similar across all groups at 12- and 28-weeks on the HFS diet. This finding is also surprising as these two proteins are often up or down-regulated coordinately[8]. Here, we speculate that the discordance between MAFbx/atrogin1 and MuRF-1 may indicate a more gradual, chronic trajectory toward muscle loss, when compared to severe, acute atrophy induction models (hindlimb suspension, denervation, casting)[8] that lead to rapid muscle atrophy. Furthermore, similar mRNA levels for MAFbx expression previously observed at 30-months[9], were observed after the 12-week diet intervention (5-6 months of age) in the present study, suggesting that obesity can result in changes similar to those associated with aging. The HFS obesity induction model may provide the advantage of detecting a gradual cascade of events over time, ultimately leading to intramuscular fat infiltration and disparate fibrosis by obesity responses that could be tracked, providing critical foundational knowledge regarding sarcopenic obesity.

However, decreased expression of MAFbx/atrogen1 in DIO animals after such a long period of HFS feeding, could be interpreted as protective—a potential attempt at minimizing muscle loss. Our data indicated decreased muscle fibre area in DIO-P and DIO-R animals at both time points, suggesting atrophy-related changes may have occurred by 12-weeks, and are sustained through 28-weeks, in obese animals. Furthermore, after obesity induction, DIO animals demonstrated an up-regulation of IGF-1 expression compared to chow animals, which is considered to be a primary growth factor pathway governing protein turnover in muscle[28]. IGF-1 may protect against skeletal muscle atrophy, blocking the MAFbx/atrogin-1 pathway[22], and is

known to reduce inflammation[29]. As muscle loss was likely initiated prior to 12-weeks in the present study, the up-regulation of IGF-1 expression at 12-weeks, in addition to the sustained down-regulation of MAFbx, could be interpreted as a possible physiological response to mitigate muscle atrophy and inflammation in DIO-P animals. Of note, we focused on the ubiquitin-ligase pathway for our initial effort to understand changes in muscle with DIO. Future studies will explore fibre area changes in more detail and will consider the potential role of decreases in the lysosomal pathway of protein synthesis, rather than focusing on muscle protein degradation.

Previous work suggests that lipid deposits in muscle affect function and maintenance[5]. In the present studies, despite similar levels of intramuscular fat deposition, the response to obesity yielded increases in CD68+ cell numbers and mRNA levels for inflammatory markers between DIO-P and DIO-R animals. Molecular outcomes previously measured at 9-months of age were similar in high-fat fed mice and control animals, supporting the notion that animals have achieved an altered set-point or heterostasis over time when metabolically challenged long-term[30]. Here, we contribute insight into molecular changes at earlier and later time points, namely after 12-weeks (3-months) of obesity induction with a HFS diet and after an additional 16-weeks on the diet (28-weeks/7-months total) in DIO-P and DIO-R groups. At 12-weeks, upregulation of mRNA levels for several markers (MCP-1, IGF-1, PPARγ, leptin, IP-10, IL-1β) in obese animals was observed in DIO-P animals, while only IL-1β was increased in DIO-R animals compared to chow controls. As evidenced by the local upregulation of IL-1β, coupled with the histological evidence of increased fibrosis and CD68+ cell number, the muscles in our study were likely affected by low-level chronic inflammation. Sarcopenic obesity[31], a condition that results from the compounded effects of obesity on age-dependent decline in muscle structure and strength, is not well understood. However, an increase in pro-inflammatory cytokine levels

has been implicated[32] Therefore, we speculate that the levels of IL-1β and the metabolic challenge may have contributed to similar intramuscular fat deposition in DIO-P and DIO-R animals. The present study was not designed to address which factors were responsible for the dysregulation in tissue homeostasis that led to the observed compromise of muscle structural integrity and from what tissues these biomarkers may have originated (intramuscular fat or muscle).

Interesting questions emerge regarding the differences in intramuscular inflammation observed at 12-weeks. Up-regulation of the adipocyte lineage marker PPARγ, and proinflammatory markers produced by fat cells (leptin, IP-10), are consistent with the intramuscular fat measured in the present study in DIO-P animals[33], but not DIO-R animals, suggesting altered activation of the fat tissue within the VL muscles of these groups. Further, the inflammatory changes in DIO-P animals were consistent with previously reported changes in sarcopenic muscles (i.e. increased IL-1β, MCP-1)[34]. Leptin is one pro-inflammatory marker of interest in several musculoskeletal and rheumatic diseases, and with obesity. In muscle however, leptin appears to influence signaling pathways that promote muscle regeneration, suggesting an important role in skeletal muscle maintenance[5]. Low-level chronic inflammation from metabolic dysfunction, and leptin, can affect homeostasis of tissue-resident cells (macrophages, adipocytes, stem cells)[32]. In the present study, the combination of increases in leptin and pro-inflammatory cells, may have contributed to the increases in fibrosis in DIO-P animals. Together with the elevation of several pro-inflammatory markers in the muscle of DIO-P animals, leptin may be playing a pro-inflammatory role, as the VL mRNA levels for leptin were markedly higher in DIO-P animals compared to DIO-R, and compared to mRNA levels for other proinflammatory markers in DIO-P animals.

Furthermore, muscles may be attempting to regulate this pro-inflammatory environment, as evidenced by adiponectin up-regulation within the DIO-P VL muscles[35]. Adiponectin generally attenuates inflammatory responses. Leptin, however, far exceeded the relative fold changes for adiponectin, suggesting that leptin may be playing a considerable pro-inflammatory role in this model. DIO-R muscles did not demonstrate the same up-regulation of pro- or anti-inflammatory mediators, or CD68+ cells, suggesting a possible protective mechanism in muscles of DIO-R animals. These findings further underscore the importance of evaluating obesity prone and resistant animals. We suggest that the response to obesity exhibited in DIO-R animals may provide novel insight into partial protective mechanisms against muscular inflammation and structural alterations.

Monocyte chemoattractant protein-1 (MCP-1)/CCL2 is typically produced in response to oxidative stress, various cytokines (TNF-α, IL-1β, IL-6) and growth factors[36], and is a potent chemokine that promotes the chemotaxis of monocytes [36]. MCP-1/CCL2 is produced by numerous tissues and cells, including macrophages. Through the recruitment of macrophages, MCP-1/CCL2 plays a critical role in the repair and regeneration of skeletal muscle[37]. Sustained increased levels of MCP-1/CCL2, and the presence of pro-inflammatory macrophages, are associated with systemic inflammation in the obese population, and are linked to insulin sensitivity[38]. In fact, MCP-1/CCL2 and its receptor have been shown to increase sharply within just three days of high fat feeding in mice, resulting in a significant increase in pro-inflammatory macrophages in skeletal muscle after 10 weeks, suggesting that MCP-1/CCL2 could be a marker of early change with metabolic challenge[24]. Previously, MCP-1/CCL2 levels were shown to be increased in sarcopenic obese patients, supporting a potential link between chronic serum inflammation and subsequent muscle loss[39]. Elevated levels of MCP-1/CCL2 mRNA levels in

DIO-P animals, and increased numbers of CD68+ cells, in the present study suggest a low-level pro-inflammatory environment within the muscle. Considering the critical role that CCL2 plays in the recruitment of innate immune cells for the repair and regeneration of muscle, it is difficult to conclude whether the absence of MCP-1/CCL-2 serves as a harmful or protective effect in DIO-R animals. More investigation is needed to understand a beneficial threshold for MCP-1/CCL2, and implications of altered expression of MCP-1/CCL-2, in repair and regeneration in this model.

By understanding the protective effects of obesity resistance, inflammatory modulation may be possible. Future studies will focus on short-term metabolic challenges during the obesity induction period to clarify the time course of intramuscular fat accumulation, atrophy marker fluctuation, fibrosis and inflammation to better understand these complex relationships. Moreover, the involvement of neural and vascular components in obesity-associated alterations are emerging as areas of interest in fat cell activation and function[40], and should also be investigated in this context.

There are a number of limitations to this work. As previously reported, an *a priori* power calculation resulted in the use of a minimal number of animals/group for these studies[14]. Future work aims to include fewer groups, with increased numbers of animals per group. Also, the vastus lateralis is a mixed muscle comprised of fast twitch oxidative glycolytic and fast twitch glycolytic fibres, and very few slow twitch oxidative fibres. Therefore, we cannot generalize our findings to a muscle that is predominantly fast or slow twitch. As predominantly slow twitch muscles contain higher numbers of satellite cells per fibre, and chronic inflammation may have significant effects on these progenitor cells, and muscle fibre type may be critical in the regeneration process[5].

Also, intramuscular fat was identified using a specific stain for neutral lipids (ORO). There could be non-neutral lipids contributing to the intramuscular fat that were not captured by our assessments. Moreover, histological assessments of fibrosis and CD68+ cells were completed only at 12- and 28-weeks post DIO. Immediate, acute inflammatory changes cannot be deduced from the results of this study, but may be critical in the changes described here. Furthermore, it is unclear if fat infiltration, inflammatory changes, and resultant fibrosis within the muscle affect subsequent muscle function. Ongoing studies are aimed at evaluating the functional adaptations of altered muscle structure due to obesity-associated alterations in muscle structural integrity, and future studies will focus on short-term diet-induced muscle alterations.

## Conclusion

Similar to humans, Sprague-Dawley rats are heterogeneous in their response to obesity. We illustrate that obesity responses are associated with increased degenerative changes in muscle structural integrity. Furthermore, obesity may induce muscular changes similar to aging before the culmination of the 12-week obesity induction period. Studying DIO-R animals in conjunction with DIO-P using this HFS diet-induced obesity model may facilitate our understanding of inflammatory mechanisms with obesity development, and provide valuable mechanistic insight into the relationship between obesity response and a spectrum of chronic diseases, such as sarcopenic obesity and osteoarthritis.

**Acknowledgements**

We thank Andrew Sawatsky and Dr. Timothy Leonard for assistance in tissue and data collection. We also wish to thank Carol Hewitt for excellent technical assistance with qPCR studies. Further, we wish to thank members of the Alberta Innovates Health Solutions Team in Osteoarthritis, and Dr. Cyril Frank for thoughtful discussion around data interpretation. We also acknowledge Azim Jinha for help with graphic design.

**Role of the Funding Source** This work was supported by the Canadian Institutes of Health Research # RT736475 and MOP 115076, the Canada Research Chair Programme, the Alberta Innovates Health Solutions Osteoarthritis Team Grant, Alberta Innovates Health Solutions, and the Killam Foundation. The funding agencies listed here had no role in the project design, execution, analysis, or manuscript drafting and submission.

**Disclosure:** The authors do not have any conflicts of interest to disclose.

## References


1. Anandacoomarasamy A, Fransen M, March L. 2009. Obesity and the musculoskeletal system. [Internet].Curr. Opin. Rheumatol. 21(1):71–7[cited 2015 Oct 3 ] Available from: http://www.ncbi.nlm.nih.gov/pubmed/19093327.

2. Gregor MF, Hotamisligil GS. 2011. Inflammatory mechanisms in obesity. [Internet].Annu. Rev. Immunol. 29:415–45[cited 2014 Jan 10 ] Available from: http://www.ncbi.nlm.nih.gov/pubmed/21219177.

3. Mihalko WM, Bergin PF, Kelly FB, Canale ST. 2014. Obesity, Orthopaedics, and Outcomes. [Internet].J. Am. Acad. Orthop. Surg. 22(11):683–690[cited 2015 Aug 7 ] Available from: http://www.jaaos.org/content/22/11/683.abstract.

4. Tidball JG. 2005. Inflammatory processes in muscle injury and repair. [Internet].Am. J. Physiol. Regul. Integr. Comp. Physiol. 288(2):R345–53[cited 2015 Apr 2 ] Available from: http://ajpregu.physiology.org/content/288/2/R345.

5. Akhmedov D, Berdeaux R. 2013. The effects of obesity on skeletal muscle regeneration. [Internet].Front. Physiol. 4:371[cited 2015 Jul 31 ] Available from: http://www.pubmedcentral.nih.gov/articlerender.fcgi?artid=3865699&tool=pmcentrez&rendertype=abstract.

6. Addison O, Drummond MJ, LaStayo PC, et al. 2014. Intramuscular fat and inflammation differ in older adults: the impact of frailty and inactivity. [Internet].J. Nutr. Health Aging 18(5):532–8[cited 2014 Nov 18 ] Available from: http://www.ncbi.nlm.nih.gov/pubmed/24886741.

7. Fellner C, Schick F, Kob R, et al. 2014. Diet-Induced and Age-Related Changes in the Quadriceps Muscle: MRI and MRS in a Rat Model of Sarcopenia. [Internet].Gerontology 60(6):530–8[cited 2014 Nov 18 ] Available from: http://www.ncbi.nlm.nih.gov/pubmed/24924578.

8. Bodine SC, Latres E, Baumhueter S, et al. 2001. Identification of ubiquitin ligases required for skeletal muscle atrophy.Science 294(5547):1704–1708.

9. Edstrom E, Altun M, Hagglund M, Ulfhake B. 2006. Atrogin-1/MAFbx and MuRF1 Are Downregulated in Aging-Related Loss of Skeletal Muscle [Internet].Journals Gerontol. Ser. A Biol. Sci. Med. Sci. 61(7):663–674[cited 2015 Apr 1 ] Available from: http://biomedgerontology.oxfordjournals.org/content/61/7/663.full.

10. Lee S, Kim T-N, Kim S-H. 2012. Sarcopenic obesity is more closely associated with knee osteoarthritis than is nonsarcopenic obesity: a cross-sectional study. [Internet].Arthritis Rheum. 64(12):3947–54[cited 2013 Dec 14 ] Available from: http://www.ncbi.nlm.nih.gov/pubmed/23192792.

11. Turpin SM, Ryall JG, Southgate R, et al. 2009. Examination of "lipotoxicity" in skeletal muscle of high-fat fed and ob/ob mice. [Internet].J. Physiol. 587(Pt 7):1593–605[cited 2015 Mar 16 ] Available from: http://www.pubmedcentral.nih.gov/articlerender.fcgi?artid=2678228&tool=pmcentrez&rendertype=abstract.

12. Collins KH, Paul HA, Reimer RA, et al. 2015. Relationship between Inflammation, the Gut Microbiota, and Metabolic Osteoarthritis Development: Studies in a Rat Model.Osteoarthr. Cartil. 23(11):1989–1998.

13. Schemmel R, Mickelsen O, Tolgay Z. 1969. Dietary obesity in rats: influence of diet, weight, age, and sex on body composition. [Internet].Am. J. Physiol. 216(2):373–9[cited 2013 Dec 14 ]

Available from: http://www.ncbi.nlm.nih.gov/pubmed/5766993.

14. Collins KH, Hart DA, Reimer RA, et al. 2015. Response to Diet-Induced Obesity Produces Time-dependent Induction and Progression of Metabolic Osteoarthritis in Rat Knees.J. Orthop. Res. In Press.

15. Cardinale J, Paul G, Sbalzarini IF. 2012. Discrete region competition for unknown numbers of connected regions. [Internet].IEEE Trans. Image Process. 21(8):3531–45[cited 2016 Feb 26 ] Available from: http://www.ncbi.nlm.nih.gov/pubmed/22481820.

16. Jin Z, Ng MK. 2014. A contrast maximization method for color-to-grayscale conversion [Internet].Multidimens. Syst. Signal Process. 26(3):869–877[cited 2016 Feb 26 ] Available from: http://dl.acm.org/citation.cfm?id=2801483.2801489.

17. Frangi A., Niessen WJ, Vincken KL, and Viergever MA. 1988. Multiscale vessel enhancement filtering. 130–137 p.

18. Antiga L. 2007. Generalizing vesselness with respect to dimensionality and shape [Internet].OR Insight [cited 2016 Feb 26 ] Available from: https://www.researchgate.net/publication/28359013_Generalizing_vesselness_with_respect_to_dimensionality_and_shape.

19. Waters-Banker C, Butterfield TA, Dupont-Versteegden EE. 2014. Immunomodulatory effects of massage on nonperturbed skeletal muscle in rats. [Internet].J. Appl. Physiol. 116(2):164–75[cited 2016 Feb 10 ] Available from: http://www.pubmedcentral.nih.gov/articlerender.fcgi?artid=3921362&tool=pmcentrez&rendertype=abstract.

20. Reno C, Marchuk L, Sciore P, et al. 1997. Rapid isolation of total RNA from small samples of hypocellular, dense connective tissues. [Internet].Biotechniques 22(6):1082–6[cited 2015 Apr 24 ] Available from: http://www.ncbi.nlm.nih.gov/pubmed/9187757.

21. Hart DA, Achari Y. 2009. Alterations to cell metabolism in connective tissues of the knee after ovariohysterectomy in a rabbit model: are there implications for the postmenopausal athlete? [Internet].Br. J. Sports Med. 44(12):867–871[cited 2015 Apr 13 ] Available from: http://www.ncbi.nlm.nih.gov/pubmed/19136500.

22. Stitt TN, Drujan D, Clarke BA, et al. 2004. The IGF-1/PI3K/Akt Pathway Prevents Expression of Muscle Atrophy-Induced Ubiquitin Ligases by Inhibiting FOXO Transcription Factors [Internet].Mol. Cell 14(3):395–403[cited 2015 Apr 13 ] Available from: http://www.sciencedirect.com/science/article/pii/S1097276504002114.

23. Friedman JM, Halaas JL. 1998. Leptin and the regulation of body weight in mammals. [Internet].Nature 395(6704):763–70[cited 2014 Dec 1 ] Available from: http://www.ncbi.nlm.nih.gov/pubmed/9796811.

24. Fink LN, Costford SR, Lee YS, et al. 2014. Pro-inflammatory macrophages increase in skeletal muscle of high fat-fed mice and correlate with metabolic risk markers in humans. [Internet].Obesity (Silver Spring). 22(3):747–57[cited 2015 Aug 3 ] Available from: http://www.ncbi.nlm.nih.gov/pubmed/24030890.

25. Tardif N, Salles J, Guillet C, et al. 2014. Muscle ectopic fat deposition contributes to anabolic resistance in obese sarcopenic old rats through eIF2α activation.Aging Cell 13(6):1001–11.

26. Divoux A, Tordjman J, Lacasa D, et al. 2010. Fibrosis in human adipose tissue: composition, distribution, and link with lipid metabolism and fat mass loss. [Internet].Diabetes 59(11):2817–25[cited 2015 Nov 17 ] Available from:

http://diabetes.diabetesjournals.org/content/59/11/2817.short.

27. Inoue M, Jiang Y, Barnes RH, et al. 2013. Thrombospondin 1 mediates high-fat diet-induced muscle fibrosis and insulin resistance in male mice. [Internet].Endocrinology 154(12):4548–59[cited 2015 Sep 21 ] Available from: http://www.pubmedcentral.nih.gov/articlerender.fcgi?artid=3836064&tool=pmcentrez&rendertype=abstract.

28. Bodine SC, Stitt TN, Gonzalez M, et al. 2001. Akt/mTOR pathway is a crucial regulator of skeletal muscle hypertrophy and can prevent muscle atrophy in vivo. [Internet].Nat. Cell Biol. 3(11):1014–9[cited 2015 Sep 30 ] Available from: http://dx.doi.org/10.1038/ncb1101-1014.

29. Sukhanov S, Higashi Y, Shai S-Y, et al. 2007. IGF-1 reduces inflammatory responses, suppresses oxidative stress, and decreases atherosclerosis progression in ApoE-deficient mice. [Internet].Arterioscler. Thromb. Vasc. Biol. 27(12):2684–90[cited 2015 Sep 30 ] Available from: http://www.ncbi.nlm.nih.gov/pubmed/17916769.

30. Lee S-R, Khamoui A V, Jo E, et al. 2015. Effects of chronic high-fat feeding on skeletal muscle mass and function in middle-aged mice. [Internet].Aging Clin. Exp. Res. [cited 2015 Mar 27 ] Available from: http://link.springer.com/10.1007/s40520-015-0316-5.

31. Lutz CT, Quinn LS. 2012. Sarcopenia, obesity, and natural killer cell immune senescence in aging: altered cytokine levels as a common mechanism. [Internet].Aging (Albany. NY). 4(8):535–46[cited 2015 Apr 17 ] Available from: http://www.pubmedcentral.nih.gov/articlerender.fcgi?artid=3461341&tool=pmcentrez&rendertype=abstract.

32. Kob R, Bollheimer LC, Bertsch T, et al. 2014. Sarcopenic obesity: molecular clues to a better understanding of its pathogenesis? [Internet].Biogerontology [cited 2014 Nov 10 ] Available from: http://www.ncbi.nlm.nih.gov/pubmed/25376109.

33. Christodoulides C, Lagathu C, Sethi JK, Vidal-Puig A. 2009. Adipogenesis and WNT signalling. [Internet].Trends Endocrinol. Metab. 20(1):16–24[cited 2014 Jun 2 ] Available from: http://www.ncbi.nlm.nih.gov/pubmed/19008118.

34. Chung HY, Cesari M, Anton S, et al. 2009. Molecular inflammation: underpinnings of aging and age-related diseases. [Internet].Ageing Res. Rev. 8(1):18–30[cited 2015 Sep 17 ] Available from: http://www.pubmedcentral.nih.gov/articlerender.fcgi?artid=3782993&tool=pmcentrez&rendertype=abstract.

35. Ouchi N, Walsh K. 2007. Adiponectin as an anti-inflammatory factor [Internet].Clin. Chim. Acta 380(1-2):24–30[cited 2015 Sep 29 ] Available from: http://www.pubmedcentral.nih.gov/articlerender.fcgi?artid=2755046&tool=pmcentrez&rendertype=abstract.

36. Deshmane SL, Kremlev S, Amini S, Sawaya BE. 2009. Monocyte chemoattractant protein-1 (MCP-1): an overview. [Internet].J. Interferon Cytokine Res. 29(6):313–26[cited 2015 Aug 24 ] Available from: http://www.pubmedcentral.nih.gov/articlerender.fcgi?artid=2755091&tool=pmcentrez&rendertype=abstract.

37. Martinez CO, McHale MJ, Wells JT, et al. 2010. Regulation of skeletal muscle regeneration by CCR2-activating chemokines is directly related to macrophage recruitment. [Internet].Am. J. Physiol. Regul. Integr. Comp. Physiol. 299(3):R832–42[cited 2015 Sep 15 ] Available from: http://www.pubmedcentral.nih.gov/articlerender.fcgi?artid=2944434&tool=pmcentrez&rendertype=abstract.

38. Sell H, Eckel J. 2007. Monocyte chemotactic protein-1 and its role in insulin resistance. [Internet].Curr. Opin. Lipidol. 18(3):258–62[cited 2015 Sep 15 ] Available from: http://www.ncbi.nlm.nih.gov/pubmed/17495598.

39. Lim JP, Leung BP, Ding YY, et al. 2015. Monocyte chemoattractant protein-1: a proinflammatory cytokine elevated in sarcopenic obesity. [Internet].Clin. Interv. Aging 10:605–9[cited 2015 Apr 9 ] Available from: http://www.ncbi.nlm.nih.gov/pubmed/25848236.

40. Zeng W, Pirzgalska RM, Pereira MMA, et al. 2015. Sympathetic Neuro-adipose Connections Mediate Leptin-Driven Lipolysis [Internet].Cell 163(1):84–94[cited 2015 Sep 24 ] Available from: http://www.cell.com/article/S0092867415011071/fulltext.

552 **Figure Legends:**

553 **Figure 1A**: Body mass is increased for DIO-P animals at both time points compared to resistant
554 and chow animals ($p<0.05$). Resistant and chow animals have similar body mass at both time
555 points measured. Data are shown as means ± SE, at each time point, and * indicates $p<0.05$
556 between prone compared to resistant and chow.

557 **Figure 1B**: Graded increases in body fat were observed at both time points. At 12- and 28-
558 weeks, prone animals had increased body fat compared to both resistant ($p=0.026$) and chow
559 animals ($p=0.001$), and resistant animals had more body fat compared to chow ($p=0.005$). Data
560 are presented as mean ± at each time point. * indicates $p<0.05$ for compared to chow, # indicates
561 $p<0.05$ for prone compared to resistant.

562 **Figure 2A**: Relative muscle wet mass compared to body mass across all groups was similar at
563 both time points. DIO-P had the lowest sarcopenia index, or relative muscle mass, at both time
564 points compared to both DIO-R (# indicates $p<0.05$ compared to DIO-R) and chow (* indicates
565 $p<0.05$ compared to chow). Data are shown as raw values within groups at both time points.

566 **Figure 2B**: Vastus lateralis muscle mass was decreased across all obese animals at both time
567 points, compared to their respective chow-fed control group. Data are shown as means ± SE.
568 Post obesity induction 12-week animals are shown in grey, where * indicates significant
569 differences compared to chow ($p<0.05$) at 12-weeks. Post adaptive period 28-week animals are
570 shown in black, where # indicates significant differences at 28-weeks compared to chow
571 ($p<0.05$).

572 **Figure 3A**: OilRedO staining for one representative slide from each group at 12 and 28-weeks.
573 Black scale bar represents 100µm, images taken at 100x magnification.

574 **Figure 3B**: Intramuscular fat percentage was similar between DIO-P and DIO-R animals, and
575 greater than chow, at both time points. * indicates $p<0.05$ compared to 12-week chow animals, #
576 indicates $p<0.05$ compared to 28-week chow animals. Data are shown as means ± SE.

577 **Figure 3C**: Picrosirius red staining for one representative slide from each group at 12 and 28-
578 weeks. Black scale bar represents 100µm, images taken at 100x magnification.

579 **Figure 3D**: VL Fibrosis was increased in DIO-P animals compared to DIO-R animals, and in
580 DIO-R animals compared to Chow at 12-weeks. At 28-weeks, VL fibrosis was similar between
581 DIO-P and DIO-R animals and greater than chow. ‡ indicates $p<0.05$ compared to DIO-R and
582 chow animals;* indicates $p<0.05$ compared to 12-week chow animals, # indicates $p<0.05$
583 compared to 28-week chow animals. Data are shown as means ± SE.

584 **Figure 3E**: CD68+ cell staining for one representative slide from each group at 12 and 28-
585 weeks. White scale bars represent 100µm, images taken at 200x magnification.

**Figure 3F**: VL CD68+ cell number was increased in DIO-P animals compared to DIO-R, and in DIO-R animals compared to Chow at 12-weeks. At 28-weeks, VL CD68+ cell number was similar between DIO-P and DIO-R animals and greater than chow. ‡ indicates $p<0.05$ compared to DIO-R and chow animals;* indicates $p<0.05$ compared to 12-week chow animals, # indicates $p<0.05$ compared to 28-week chow animals. Data are shown as means ± SE.

**Figure 4**: A preliminary analysis of muscle fibres revealed decreased fibre area in DIO-P and DIO-R animals compared to chow at both 12- and 28-weeks. All 12-week groups included n=3 animals/group (chow=551 fibres, DIO-R=863 fibres, DIO-P=679 fibres). 28-week animals included n=2 animals/group in chow (n=255 fibres) and DIO-R animals (n=424 fibres), and n=3/group in DIO=P animals (n=627 fibres). Data are shown as box-plots where whiskers indicate minimum and maximum values, boxes demonstrate the interquartile range from Q1-Q3, and median values are expressed. * indicates $p<0.05$ compared to chow control-diet animals at each time-point.

**Figure 5A**: Relationships between body fat percentage and vastus lateralis (VL) mass at 12- and 28-weeks across all animals; r=-0.50, p=0.03.

**Figure 5B**:Relationships between body fat percentage and vastus lateralis (VL) average OilRedO staining to represent intramuscular fat at 12- and 28-weeks across all animals; 12-weeks:r=0.79, $p<0.001$; r=28-weeks: r=0.84, $p<0.001$.

**Figure 5C**: Relationships between vastus lateralis (VL) average oil red O staining to represent intramuscular fat and VL fibrosis at 12- and 28-weeks across all animals; 12-weeks r=0.73, p=0.001; 28-weeks r=0.63, p=0.003.

**Figure 6**: MAFbx/atrogin1, but not MURF, is down-regulated in all DIO animals at both time points with exposure to high-fat, high-sucrose diet. Data are presented normalized to chow control diet mRNA levels, and graphed as means ± SE. * indicates $p<0.05$ compared to 12-week chow animals.

**Figure 7**: Relevant molecular markers associated with muscle atrophy are differentially up-regulated across all obesity prone (P) animals at 12-weeks compared to obesity resistant (R). Data are presented normalized to chow-fed control mRNA levels, and graphed as means ± SE. * indicates $p<0.05$ DIO-P compared to DIO-R; # indicates $p<0.05$ compared to chow control-diet animals.

**Figures and Tables:**

Figure 1a:

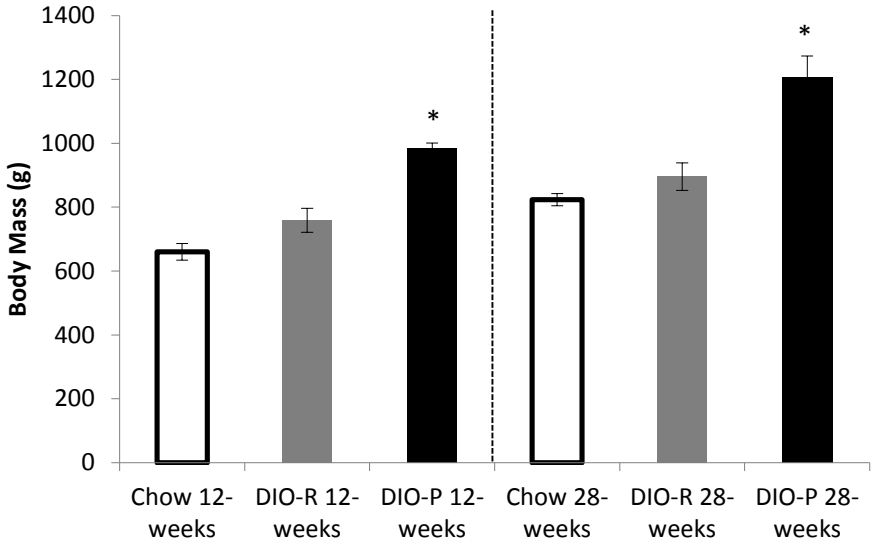


Figure 1b:

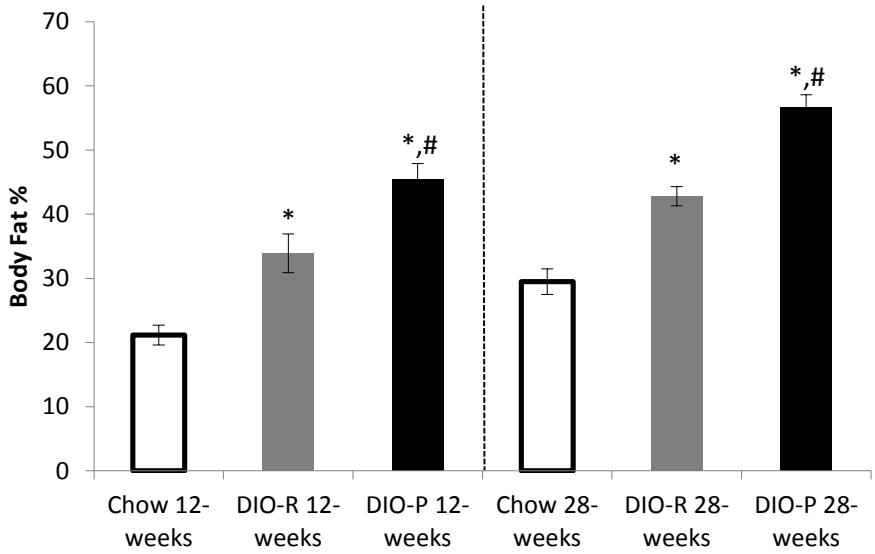

Figure 2a:

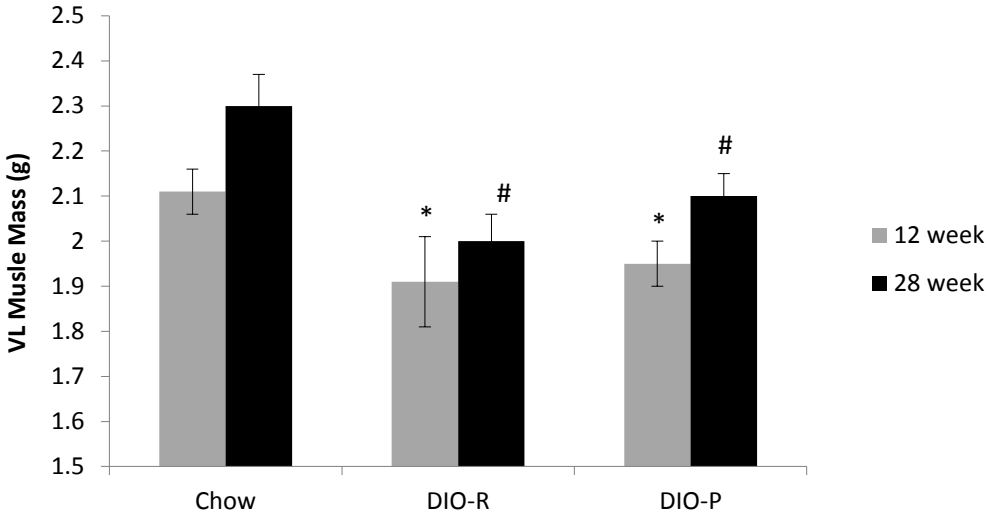


Figure 2b:

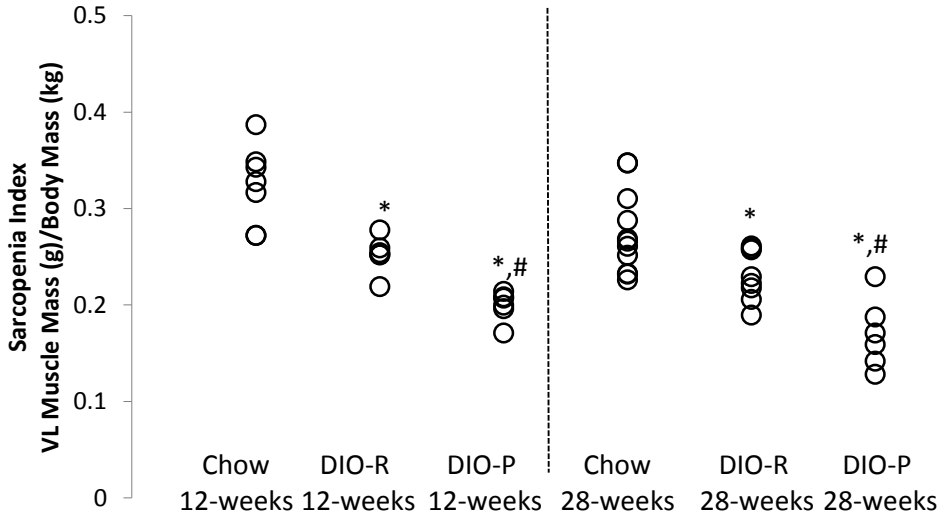

633 Figure 3:

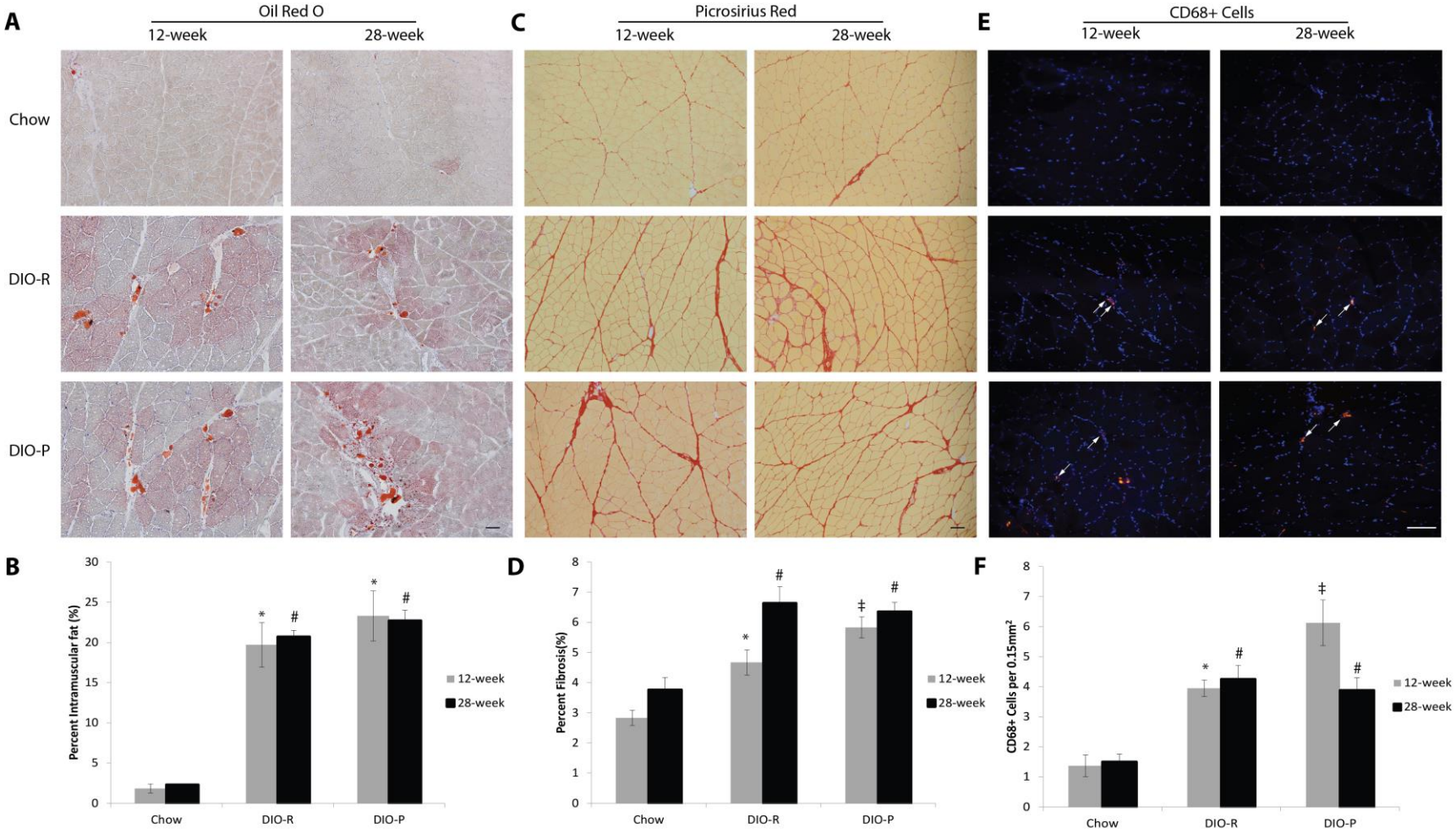


634

635 Figure 4:

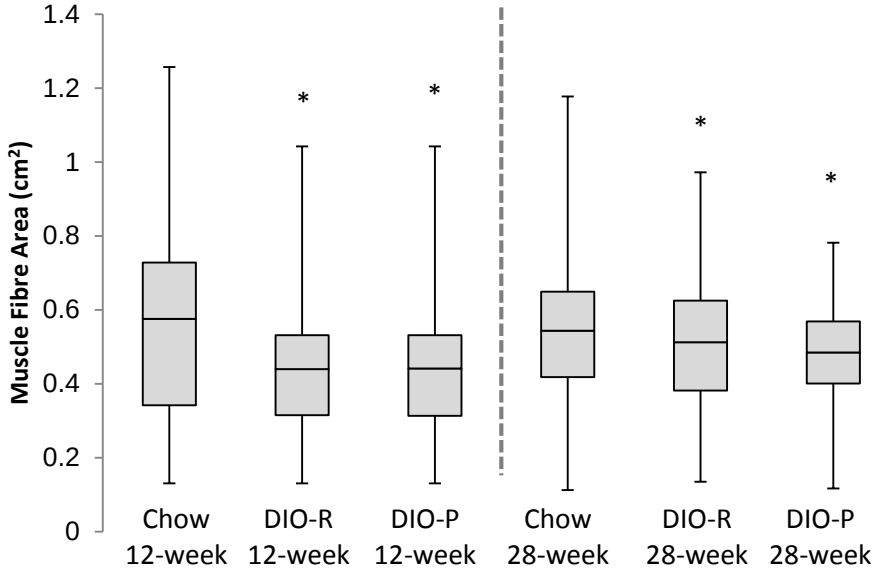


636

Figure 5a:

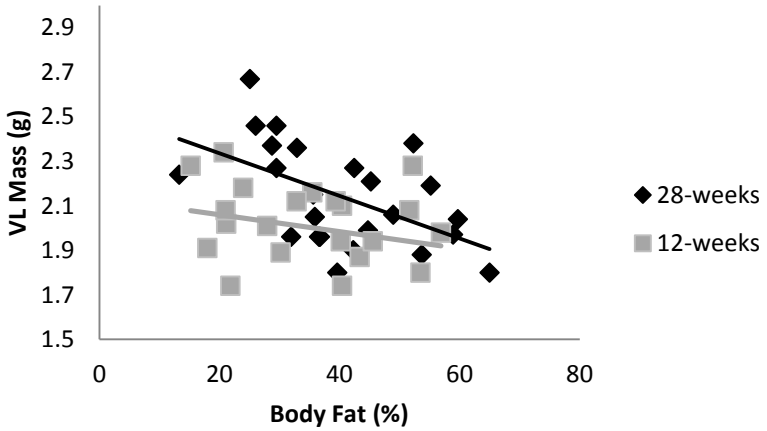


Figure 5b:

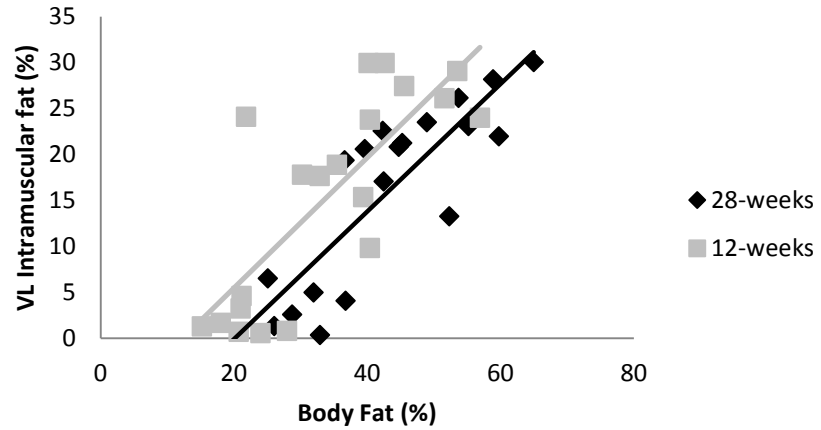


Figure 5c:

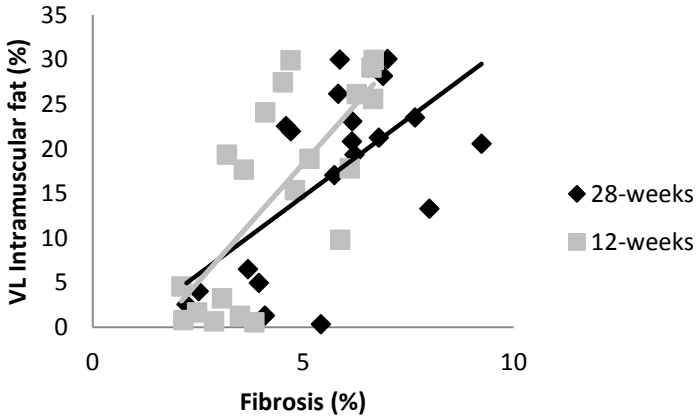

Figure 6:

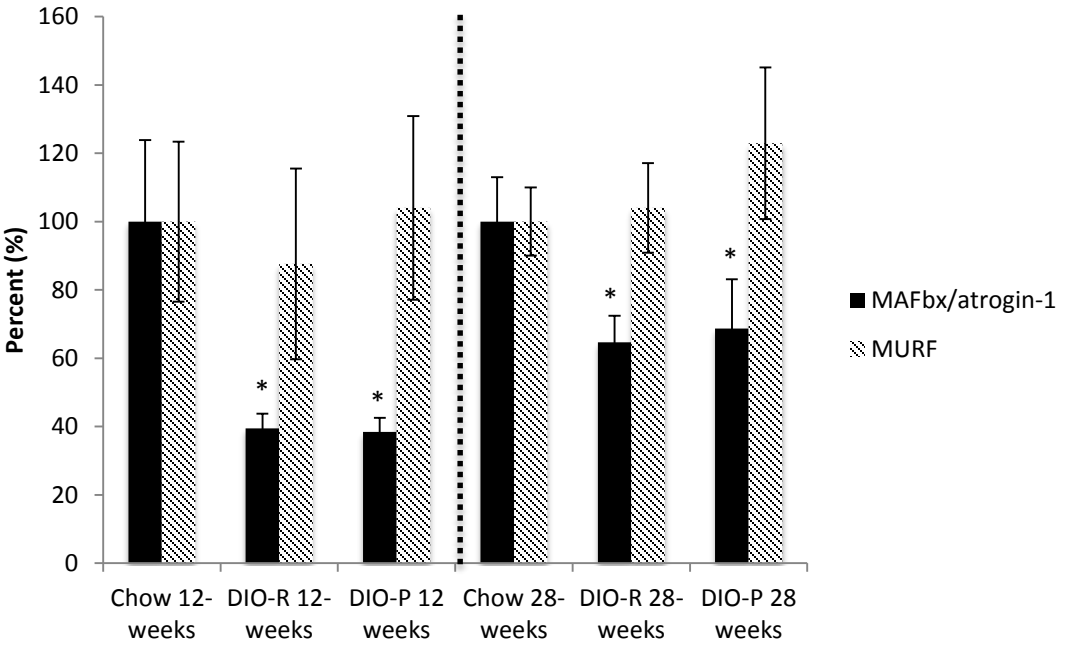
160
140
120
100
80
60
40
20
0
Percent (%)
*
*
*
*
Chow 12-weeks
DIO-R 12-weeks
DIO-P 12 weeks
Chow 28-weeks
DIO-R 28-weeks
DIO-P 28 weeks
MAFbx/atrogin-1
MURF

Table 1: Ratios of mRNA levels between DIO-P: DIO-R animals suggest obesity-response dependence among pro-inflammatory, anti-inflammatory, and growth factor primers, but not atrophy primers, evaluated in these studies; * p<0.05; **p<0.01, ***p<0.001.

| Gene | Ratio DIO-P: DIO-R | Ratio DIO-P: chow | Ratio DIO-R: chow |
|---|---|---|---|
| **Leptin** | 5.1** | 16.7** | 3.4 |
| **Adiponectin** | 3.2** | 2.9* | 0.9 |
| **IP-10** | 2.4* | 2.5* | 1.1 |
| **IGF-1** | 2.1 (p=0.08) | 3.0** | 1.9 |
| **MCP-1** | 2.2* | 2.5** | 1.1 |
| **PPARϒ** | 1.4* | 1.9* | 1.4 |
| **IL-1β** | 1.8* | 3.1** | 1.7* |
| **MuRF-1** | 1.0 | 0.4* | 0.4* |
| **MAFbx/atrogin-1** | 1.1 | 0.6* | 0.7* |

678 Figure 7:

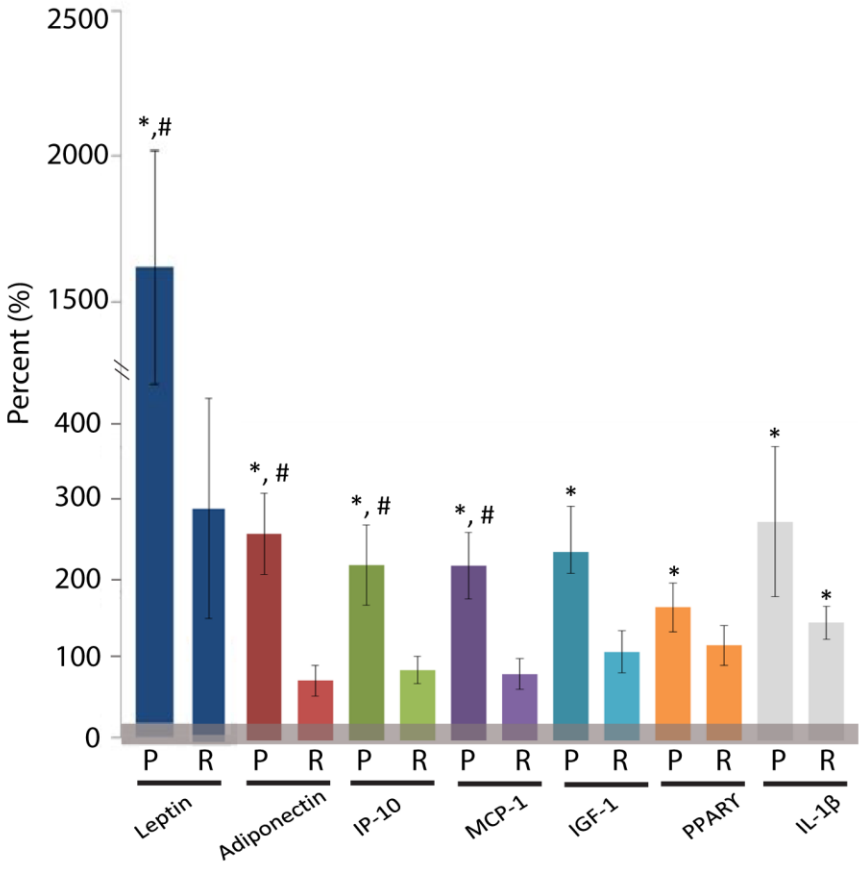


679

680

**Supplementary Table 1**: qPCR Primer Sequences

| Primer | Forward Sequence | Reverse Sequence | Origin |
|---|---|---|---|
| MCP-1 | ACT ATG CAG GTC TCT GTC AC | TGC CAG TGA ATG AGT AGC AG | M54771 |
| IGF-1 | GCA TTG TGG ATG AGT GTT GC | GGT CTT GTT TCC TGC ACT TC | X06043 |
| PPARϒ | CTT GGC CAT ATT TAT AGC TGT CAT TAT T | TGT CCT CGA TGG GCT TCA C | NM_013124 |
| Leptin | CCT GTG GCT TTG GTC CTA TCT G | CTG CTC AAA GCC ACC ACC TCT G | NM_013076 |
| IP-10 | CAA GGC TTC CCA ATT CTC | ACC TGG ACT GCA TTT GA | U22520 |
| IL-1β | AAC CTG CTG GTG TGT GAC GTT C | CAG CAC GAG GCT TTT TTG TTG T | NM_008361 |
| Visfatin | CAC TCA GCA TTC AGC GTA GG | GCC AGT GCT GCC GTC ATA AT | NM_144744 |
| Adiponectin | TCA CCC CAG ATG ACA GGA AA | CAT GAC ACA TTC CAC CAC CA | NM_053365 |

k